Single Molecule Detection and Photochemistry on a Surface Using Near-Field Optical Excitation

W. Patrick Ambrose,* Peter M. Goodwin,* John C. Martin,† and Richard A. Keller*

Los Alamos National Laboratory, Los Alamos, New Mexico 87545

(Received 20 October 1993)

We report the first photobleaching experiments of single molecules on a surface. Single molecules of rhodamine 6G are detected on a silica surface under ambient conditions using near-field scanning optical microscopy. Photobleaching of an individual molecule appears as an abrupt disappearance of fluorescence after seconds of constant excitation. Other reversible, upward and downward changes in fluorescence are observed, possibly due to reorientation of molecules on the surface.

PACS numbers: 78.66.Qn, 07.60.Pb, 33.50.−j, 42.81.Wg

We demonstrate that near-field scanning optical microscopy can be used to detect single, fluorescent rhodamine-6G (R-6G) molecules on a silica surface under ambient conditions and to observe the time to photobleaching for individual molecules. The key signature for single molecule detection on a surface is the characteristic nature of the fluorescence signals during photobleaching at the single molecule level; after $\sim 10^7$ optical excitations there is an abrupt, irreversible loss of fluorescence signal corresponding to a low probability chemical modification. Before the disappearance of fluoresence discrete, reversible steps in the signal are often observed, probably associated with reorientation of molecules on the surface. Detection of single molecules on a surface heralds a significant improvement in the sensitivity of optical microscopy and opens a new era in surface photochemistry and photophysics.

Optical single molecule detection (SMD) has been achieved recently in liquids [1–4] and solids [5–8]. In all previous SMD experiments, molecular excitations were produced with near diffraction limited, far-field focused laser light [1–8]. Since the signal is proportional to the irradiance at the molecule of interest (I=power/area) and the background scatter and its associated noise increase with the power, enhanced sensitivity is achieved by decreasing the area of illumination. A method for generating a subdiffraction limit spot of light at a solid surface has been demonstrated in near-field scanning optical microscopy (NSOM) [9]. NSOM is a scanned probe microscopy employing a metal coated, sharpened optical guide with a submicron optical aperture at the tip. Recent advances in tip [10] and detector [11] technology have made SMD with NSOM possible [12].

We have built an NSOM similar to those described previously for illumination mode optical imaging [9,10] and have incorporated shear force microscopy (SFM) for tip-to-surface distance regulation [10]. SFM involves oscillating the NSOM fiber ~ 5 nm transversely, damping the oscillation with tip-to-surface shear forces, and using the amplitude as feedback to the sample position for constant tip height operation. The tip oscillation was measured by focusing a 1 mW, 1.3 μm laser beam on the fiber and detecting the diffracted light with an InGaAs photodiode. The height noise was 4 nm. Continuous wave excitation light (Ar^+ laser at 514.5 nm) was coupled into a single mode optical fiber and emerged through a ~ 90 nm aperture in close proximity to the surface of a silica disk. Fluorescence from R-6G molecules on the surface was excited and collected through the substrate using a high numerical aperture, oil immersion objective (1.3 NA, 90×, Leitz Wetzlar). The excitation light was rejected with interference filters transmitting wavelengths > 520 nm. The transmitted light was spatially filtered with a 400 μm pinhole in the image plane of the objective and reimaged onto a photon counting Si avalanche photodiode (EG&G APD, ~ 18 dark counts/sec, $\sim 50\%$ detection quantum efficiency) [11]. Movement of the sample and image collection were accomplished by commercial scanning electronics (Topometrix). The far-field power at 514.5 nm, reflected from an interference filter, was monitored with an unbiased Si photodiode in a 10 Hz bandwidth. The far-field polarization state was not measured. The sample scan ranges were calibrated using Michelson interferometry, and by recording SFM images on a 1 μm grid in a metal film. NSOM probe tips were fabricated by metal coating tapered single mode fibers using techniques similar to those described previously [10]. To measure the fluorescence intensity as a function of time in photobleaching experiments, pulses from the APD were counted in a multichannel scaler with a channel advance rate set at 100 Hz (10 msec/bin). For optical alignment without photobleaching and for nonresonant heating experiments, HeNe laser light at 632.8 nm was coupled into the NSOM fiber.

R-6G on silica was chosen for demonstrating SMD in fluorescence NSOM, since many photophysical properties of this system are known [13–17]. A detailed knowledge of these properties is extremely valuable in the interpretation of these results. R-6G (Exciton, R 590 chloride) was dissolved in methanol, diluted to $10^{-8}M$, and deposited on 160 μm thick, fused silica disks by spin coating to yield an expected *average coverage* of $\sim 10^9$ R-6G/cm^2 [14], well under an estimated monolayer coverage of $\sim 10^{14}$ R-6G/cm^2 [13].

Figure 1 shows a sequence of fluorescence images taken in the same 3.3×4.7 μm region. Each image is composed

0031-9007/93/72(1)/160(4)$06.00

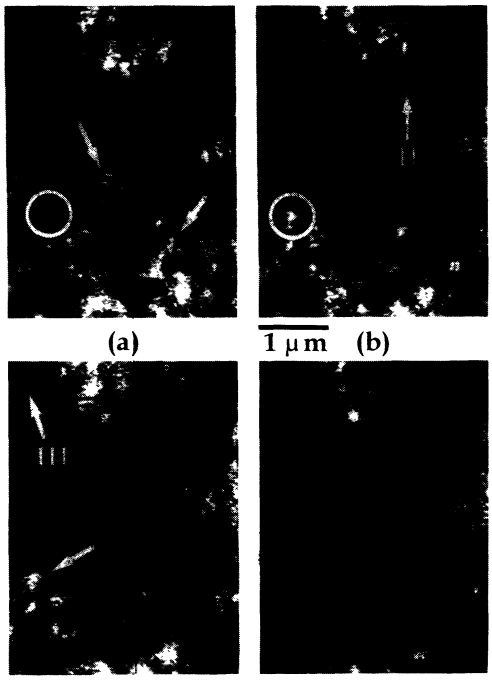

FIG. 1. A sequence of fluorescence excitation images on a dry silica surface with a submonolayer coverage of R-6G molecules. Black is dim (at the optical background level with no molecules excited) and white is bright (more molecules excited). Labeled arrows indicate photobleaching positions corresponding to curves in Fig. 2. The feature labeled II in (b) is a single R-6G molecule located with ~90 nm optical resolution.

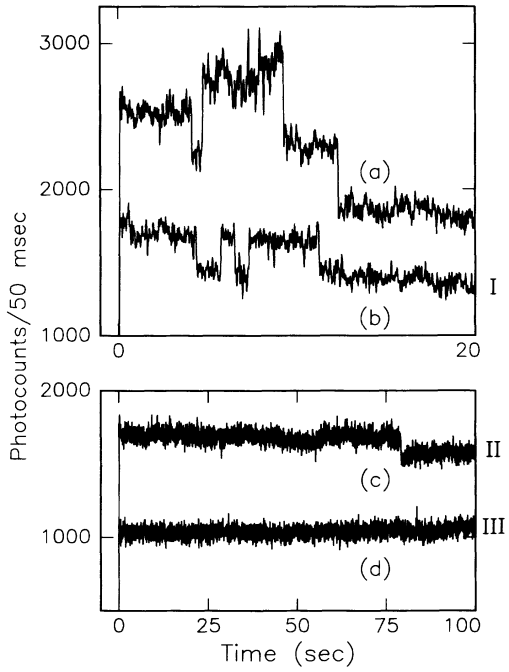

FIG. 2. Photobleaching of individual R-6G molecules on a silica surface. Traces (a)–(c) show abrupt changes in fluorescence as single molecules are reversibly altered, and then irreversibly photobleached. (d) is the unchanging background in a dark region III of Fig. 1(c). Traces labeled I–III on the right-hand side were taken at the labeled arrows in Fig. 1. Traces (a) and (c) are offset for clarity.

of 200×200 pixels scanned at 20 msec/pixel (26.7 min/image). The photon counter was operated with a count interval of 50 msec. With an input power of 0.21 mW at 514.5 nm, the far-field output power at this wavelength was 19 ± 2 nW. In image (a), the observed signal ranges from ~130 (background scatter) to ~600 photocounts/50 msec. Two images were obtained prior to image (a). Both increases and decreases in brightness were observed, e.g., portions of the top center bright region in (a) dimmed slightly and the feature labeled I brightened. The optical resolution was estimated from small features [such as II in image (b)] to be ~90 nm full width at half maximum, well under the diffraction limit for the 514.5 nm light (~240 nm).

For photobleaching, light entering the NSOM fiber was blocked, and the tip was positioned at an arrow in Fig. 1. The optical power was increased from 0.21 to 2.1 mW, and the beam was unblocked for 2 to 3 min. The beam was then blocked and the power was reduced to 0.21 mW for fluorescence image acquisition. During bleaching, the lateral drift was < 15 nm. Photobleached regions dropped to the background level. As a control, the dark region labeled III in Fig. 1(c) was irradiated and no changes were observed. Curiously, a dim region encircled in (a), which is 0.9 μm from the bleaching position I, appears brighter in image (b). This bright spot is bleached after image (c), and appears dark in (d).

Photobleaching was studied also on higher concentration samples. Silica disks spin coated with $10^{-7}M$ and $10^{-6}M$ R-6G in methanol (10× and 100× higher than in Fig. 1) show order of magnitude variations in coverage when measured on a scale of 10 μm in fluorescence NSOM. The pattern of dye coverage suggests that ~1 μm holes form in the evaporating film, often originating at ~10 nm high bumps on the silica surface. Fluorescence versus time was studied with 514.5 nm excitation light at 2 to 2.5 mW input power (≤ 180 nW in the far field. The fluorescence was observed to decay monotonically with an initial rate of ~0.1 sec^{-1}. Images obtained before and after bleaching on the higher coverage samples reveal dark, bleached spots.

Examples of the fluorescence observed during bleaching in Fig. 1 are shown in Fig. 2. Instead of smooth, monotonically decreasing curves observed for higher coverage samples, the signals in Fig. 2 display regions of approximately constant fluorescence separated by rapid downward *and* upward steps several times larger than the noise. The data in Fig. 2 were recorded in 10 msec count intervals and later convolved with a 50 msec window. The noise on short time scales is within 5% of expected

shot noise, or counting statistical noise. When the raw, unconvolved data are examined the jumps are observed to occur in ≤ 10 msec. Trace (c) shows a simple example of approximately constant fluorescence before the photobleaching step to the background level at 79 sec. As a control, trace (d), taken in a region initially at the background level, does not change throughout the 150 sec measurement. The dark areas of Fig. 1 are regions where no molecules are excited to fluorescence. Before photobleaching, traces (a) and (b) exhibit a sequence of upward and downward transitions over the first ~ 15 sec, and then execute a final downward transition to a background level that remains constant out to 150 sec. Many of the jumps before the final irreversible bleaching transition return the fluorescence signal to previous levels, i.e., some of these changes appear reversible. Since no sudden changes in excitation light level or tip height are observed during these experiments, and since the largest fluorescence jumps are 250 to 500 photocounts/50 msec (20% to 30% of the initial total signal), these fluorescence changes are intrinsic to the fluorescent species on the surface. The time from the beginning of seven traces to the final bleaching transition is $\tau_b = 45 \pm 30$ sec. The time between the 36 largest steps was observed to range from 1 to 120 sec with a mean time between steps of 15.3 sec.

We assert that the data in Figs. 1 and 2 are evidence for achieving optical single molecule detection sensitivity on a surface and the observation of photochemistry at the single molecule level. The strongest qualitative evidence is the character of the photobleaching traces at low coverage. With only a few R6-G molecules in the near-field region, the fluorescence signal is roughly constant until a single molecule undergoes a rapid change. The different brightnesses and step sizes are due to the random in-plane orientations of the transition dipoles on a glass surface [14,16,17] yielding differing rates of excitation by the electric field at the tip. The quantitative features (largest step sizes and mean time to bleaching) are also consistent with previously observed photophysical parameters for R-6G and similar laser dyes on surfaces [14,17–19].

The expected signal size from a single R-6G molecule may be estimated. The total rate of photon emission from a single molecule is $R_f = \sigma I \Phi_f / h\nu$, where σ is the absorption cross section, I is the irradiance at the molecule, Φ_f is the fluorescence quantum efficiency, and $h\nu$ is the excitation energy. An estimate for the irradiance on the surface during the photobleaching experiments, without correcting for possible near-field enhancements [9], is $I = 186 \times 10^{-9}$ W/6.6×10^{-11} cm^2 $= 2.8 \pm 0.4$ kW/cm^2, where the area was calculated using a diameter of 90 nm. Following Huston and Reimann [17], we assume σ has the value for R-6G in methanol, $\sigma = (2 \pm 0.5) \times 10^{-16}$ cm^2, $\Phi_f = 0.8 \pm 0.2$ [18], and $1/h\nu = 2.6 \times 10^{18}$ photons/W sec, to obtain a fluorescence emission rate $R_f = (1.1 \pm 0.4) \times 10^6$ photons/sec. Possible alterations of σ in the near field and Φ_f near the metal tip are not considered. From a calculated overall collection and detection efficiency of $D = 0.03 \pm 0.004$ photocounts/photon emitted, the expected single molecule signal is $R_f D = (3.3 \pm 1.3) \times 10^4$ photocounts/sec $= 1650 \pm 650$ photocounts/50 msec. Since scanner hysteresis results in positioning errors and nonoptimal excitation during photobleaching experiments, the calculation is in reasonable agreement with our assertion that the largest fluorescence jumps of ~ 500 photocounts/50 msec in Fig. 2 are due to single molecule changes.

The quantum efficiency for photobleaching Φ_b may be estimated from the measured single molecule signal of $R_f D \sim 500$ photocounts/50 msec, D and τ_b. A fluorescence trace shows single molecule fluorescence steps, but some traces [such as Fig. 2(a)] may involve more than one molecule and earlier photobleaching events are not included in the estimate of τ_b. Hence, the value for τ_b is possibly an overestimate, and $\Phi_b = \Phi_f / R_f \tau_b \sim (0.2$ to $2) \times 10^{-7}$ is possibly an underestimate by a factor of 2 or 3. A value of $\Phi_b \sim 10^{-7}$ to 10^{-6} is on the low end of the distribution of efficiencies (10^{-5} to 10^{-7}) determined from nonexponential bleaching curves for R-6G on silica [17]. This wide range of values results from the heterogeneous environments and different binding geometries on a glass [17]. The reason that molecules in Fig. 2 appear to be on the stabler end of this range is probably due to bleaching of the more labile molecules during images obtained prior to each of the photobleaching traces.

With an estimate of the single molecule signal size from Fig. 2, a reexamination of the features in Fig. 1 shows which of them result from single molecules. The images in Fig. 1 were collected with the lower input power of 0.21 mW where the single molecule fluorescence signal is expected to be ~ 50 photocounts/50 msec above background. Hence, in image (a) the signals correspond to zero molecules in dark regions at the background level of ~ 130 photocounts/50 msec up to as high as ~ 12 molecules in the brightest regions, with the average number of molecules $= 2.6$ per resolution element. Since the photobleaching curve in Fig. 2, trace (c) contains a single step downwards, the corresponding feature labeled II in Fig. 1(b) is a single molecule detected at our near-field resolution of 90 nm.

The observed coverage of $\sim 4 \times 10^{10}$ R-6G/cm^2 in this 15.5 μm^2 portion of the sample is much higher than the expected average coverage of $\sim 10^9$ R-6G/cm^2 [14]. This is consistent with the order of magnitude variations observed on higher coverage samples on a 1 to 10 μm scale noted above, and is still far below the critical concentration of 2×10^{12} R-6G/cm^2 where fluorescence is quenched by dimers [14].

Since the NSOM tip temperature increases with input power, one possibility for some of the changes observed in Figs. 1 and 2 is a sample heating effect. To test for heating effects, 632.8 nm light at which the R-6G molecules do not absorb was used to heat the tip during experiments on higher coverage samples. With 3.3 mW of input

power at 632.8 nm (180 nW transmitted into the far field), the tip was set at fixed positions on the sample for as long as 12 min. There were no observable changes in subsequent fluorescence images. We conclude that the irreversible removal of fluorescence with 514.5 nm light is a photoinduced effect and not a heating effect. Features that brighten near the bleaching position, such as the circled region in Figs. 1(a) and 1(b), may have resulted from increased thermal motion during bleaching.

We attribute the reversible changes in fluorescence to hopping motions [20] that change the molecular orientation and excitation rate. Other possibilities include (1) metastable excited states (such as photoionization and electron trapping), (2) a metastable chemical condition (such as association and dissociation of dimers), or (3) sudden changes in the glass surface structure. Further work will be required to explore these possibilities. We cannot rule out the theoretical possibility that some of these single fluorescers may be strongly optically allowed dimers or other small aggregates in previously unobserved, rare configurations on silica [21]. Electronically coupled molecules are single quantum systems and should behave in many respects as single molecules. Observed dimers and aggregates of R-6G at high concentration on silica and in sol gel films have order of magnitude reduced fluorescence yields [17], and are more photolabile than the monomers [22]. We would not expect to observe these more weakly fluorescing aggregates. Ultimately the importance of this work lies in the demonstrated ability to reveal the unique behavior of single molecules on a surface under ambient conditions, such as abrupt photobleaching and the previously unobserved reversible fluorescence jump behavior.

*Chemical Science and Technology Division.
†Life Sciences Division.

[1] E. B. Shera, N. K. Seitzinger, L. M. Davis, R. A. Keller, and S. A. Soper, Chem. Phys. Lett. **17A**, 553 (1990).
[2] C. W. Wilkerson, P. M. Goodwin, W. P. Ambrose, J. C. Martin, and R. A. Keller, Appl. Phys. Lett. **62**, 2030 (1993).
[3] M. D. Barnes, K. C. Ng, W. B. Whitten, and J. M. Ramsey, Anal. Chem. **65**, 2360 (1993).
[4] R. Rigler, J. Widengren, and Ü. Mets, in *Fluorescence Spectroscopy New Methods and Applications*, edited by O. S. Wolfbeis (Springer-Verlag, Berlin, 1993), p. 13.
[5] M. Orrit and J. Bernard, Phys. Rev. Lett. **65**, 2716 (1990).
[6] W. P. Ambrose and W. E. Moerner, Nature (London) **349**, 225 (1991).
[7] W. E. Moerner and T. Basché, Angew. Chem. **32**, 457 (1993).
[8] M. Pirotta, F. Güttler, H. Gygax, A. Renn, J. Sepiol, and U. Wild, Chem. Phys. Lett. **208**, 379 (1993).
[9] U. Dürig, D. W. Pohl, and F. Rohner, J. Appl. Phys. **59**, 3318 (1986).
[10] E. Betzig and J. K. Trautman, Science **257**, 189 (1992).
[11] L. Q. Li and L. M. Davis, Rev. Sci. Instrum. **64**, 1524 (1993).
[12] E. Betzig and R. J. Chichester (to be published).
[13] D. C. Nguyen, R. E. Muenchausen, R. A. Keller, and N. S. Nogar, Opt. Commun. **60**, 111 (1986).
[14] M. Lieberherr, C. Fattinger, and W. Lukosz, Surf. Sci. **189**, 954 (1987).
[15] F. R. Aussenegg, A. Leitner, M. E. Lippitsch, H. Reinsich, and M. Riegler, Surf. Sci. **189**, 935 (1987).
[16] H. Sano, G. Mizutani, and S. Ushioda, Surf. Sci. **223**, 621 (1989).
[17] A. L. Huston and C. T. Reimann, Chem. Phys. **149**, 401 (1991).
[18] R-6G in sol gel films has a $\Phi_f = 0.8$ [R. Reisfeld, R. Zusman, Y. Cohen, and M. Eyal, Chem. Phys. Lett. **147**, 142 (1988)]. R-6G on silica has a fluorescence lifetime (3.5 ns) close to values in solutions [17]. It is reasonable to assume that R-6G on silica also has a Φ_f similar to values in solutions of 0.8 ± 0.2 [S. A. Soper, H. L. Nutter, R. A. Keller, L. M. Davis, and E. B. Shera, Photochem. Photobiol. **57**, 972 (1993)]. See also Ref. [14].
[19] Reisfeld *et al.* (Ref. [18]).
[20] J. K. Thomas, Chem. Rev. **93**, 301 (1993).
[21] K. Kemnitz, N. Tamai, I. Yamazaki, N. Nakashima, and K. Yoshihara, J. Phys. Chem. **90**, 5094 (1986).
[22] U. Narang, F. V. Bright, and P. N. Prasad, Appl. Spect. **47**, 229 (1993).

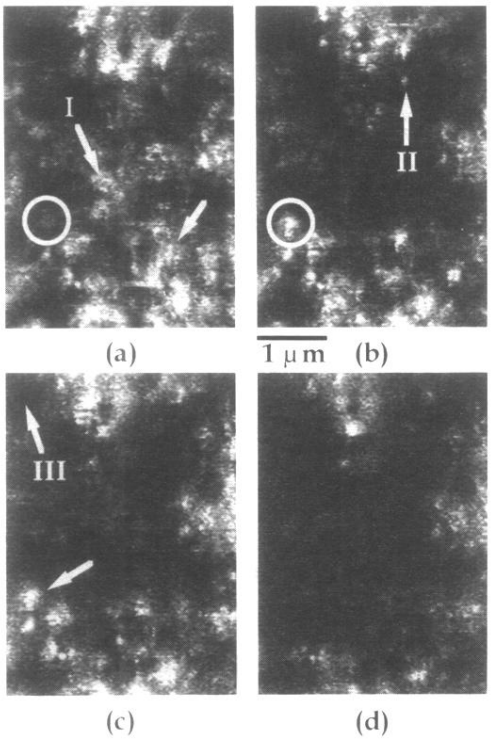

FIG. 1. A sequence of fluorescence excitation images on a dry silica surface with a submonolayer coverage of R-6G molecules. Black is dim (at the optical background level with no molecules excited) and white is bright (more molecules excited). Labeled arrows indicate photobleaching positions corresponding to curves in Fig. 2. The feature labeled II in (b) is a single R-6G molecule located with ~90 nm optical resolution.